OBSERVATION OF TRANSVERSE-LONGITUDINAL COUPLING EFFECT AT UVSOR-II

M. Shimada#, KEK, Tsukuba, 305-0801 Ibaraki, Japan
M. Katoh, M. Adachi, T. Tanikawa, S. Kimura, UVSOR, Okazaki, 444-8585, Japan
M. Hosaka, N. Yamamoto, Y. Takashima, Nagoya University, Nagoya, 464-8603, Japan
T. Takahashi, KURRI, Kumatori-cho, 590-0494, Japan

Abstract

It was theoretically predicted that, when the electron pulse length comes into the sub-picosecond range, transverse motion of the electrons is strongly coupled with the longitudinal one and makes significant effect on the pulse shape. In the experiments, a fine dip structure was created on the electron bunches circulating in a storage ring by a so-called laser bunch slicing technique and then the evolution of the structure was observed through the spectrum of the coherent synchrotron radiation (CSR). When the ring was operated in a low-alpha mode, the shape of the dip structure was oscillating with the transverse betatron frequency, which clearly indicates the existence of the longitudinal-transverse coupling effect.

INTRODUCTION

Steady state operation of short electron bunches in sub-picosecond range is critical issue for light source, aiming to sub-picosecond X-ray pulses and intense CSR in THz region. When the electron pulse length comes into the sub-picosecond range, it was theoretically predicted that transverse emittance easily affects on longitudinal one, and it leads to lengthening the electron bunch even if there is no collective effect, such as CSR wake and instability [1]. We succeeded in the observation of the longitudinal-transverse coupling effect by tracking the dip structure created on the long electron bunch by the technique called 'laser bunch slicing' at UVSOR-II [2]. The evolution of the longitudinal size of dip structure is measured turn-by-turn via CSR by utilizing Schottky diode detectors for THz region.

EXPERIMENTS SETUP

Laser Bunch Slicing

A laser pulse of sub-picosecond duration interacts with an electron bunch several tens of picoseconds long. An intense laser field modulates the energy of electrons travelling in a periodic magnetic field produced by an undulator. After the interaction, the electrons trace different orbits depending on their energy. This produces differences in orbit length, and hence in longitudinal position. As a result, the energy-modulated electrons escape their original positions and form electron fragments of a sub-picosecond duration [see Fig. 1]. At the same time, a dip structure is created in the unmodulated electron bunch. Figure 1 shows a schematic drawing of the laser bunch slicing system at UVSOR-II, which consists of a Ti:Sa laser system, an undulator, and an IR/THz beam-line [3]. In the laser system, the seed light from a mode-locked Ti:Sa laser is synchronized with the RF signal of 90.1 MHz, which picked up from the RF accelerating cavity. The pulse duration of the Ti:Sa laser can be controlled in the range from 130 fs to 1 ps by chirping using the amplifier's internal grating pair. The main parameters of the laser are listed in Table 1.

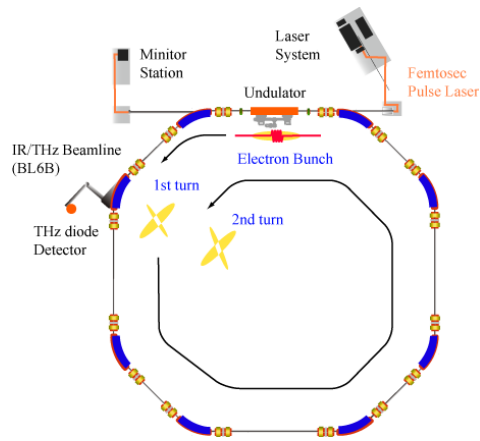

Figure 1: Schematic drawing of laser bunch slicing system at UVSOR-II and turn-by-turn CSR.

Table 1: Main Parameters of Ti:Sa Laser

Wavelength [nm]	800
Pulse energy [mJ]	2.5
Repetition rate [kHz]	1
Pulse width [ps]	0.13 - 1

Low Alpha Optics

The momentum compaction factor, α_C, is defined as follows

$$\frac{\Delta T}{T} = \alpha_C \frac{\Delta P}{P} = \alpha_C \Delta\delta \qquad (1)$$

where T, P and δ are revolution time, electron kinetic energy and electron energy deviation, respectively. The

#miho.shimada@kek.jp

longitudinal slippage due to the energy deviation is suppressed when α_C is small. Such an operation mode is called 'low alpha optics', which is important for maintaining the sub-picosecond longitudinal structure in the storage ring.

In this experiment, the ring was operated in single bunch mode, in which only one electron bunch is circulating, with two low-alpha optics with different betatron tunes of 3.53 and 3.68. Since the tune is close to the half and third resonances, we refer to the latter two as low-alpha (1/2) and low-alpha (1/3) optics. The main parameters of the low-alpha optics are compared with the normal optics in Table 2. The momentum compaction factor, α_C, of the low-alpha optics is about one-fifth that of the normal optics. The betatron and dispersion function are shown in Fig. 2.

Beamline and Detector

THz CSR was observed at the IR/THz beam-line, which is equipped with a magic mirror with large acceptance angle of 215 x 80 mrad^2. The source point is the second bending magnet from the undulator. A Schottky diode detector has a temporal response of a few hundred picoseconds and a narrow frequency bandwidth. This fast temporal response made it possible to observe THz CSR emitted by the electron bunch turn-by-turn. The diode detectors were prepared with three sensitive to frequency ranges, 11.0 - 16.6 cm^{-1} and 7.3 - 11.0 cm^{-1} (Virginia Diode Instruments, WR2.2ZBD and WR3.4ZBD), and 3.7 - 5.7 cm^{-1} (Millitech, Inc., DXP-06).

EXPERIMENTAL RESULTS

With the low alpha (1/2) optics, as shown in Fig. 3 (a) - (c), the CSR is intense at every other turns. In the middle and high-frequency ranges, it is intense at the first and third arrivals. At the low-frequency range, it could be observed up to the 11th arrival. Although the CSR at the third and fifth arrivals is intense, that of the first arrival is weak.

Table 2: Main Parameters of a Normal and Two Low-alpha Optics

	Normal	Low αc (1/2)	Low αc (1/3)
αc	0.028	0.0062	0.0047
νx	3.75	3.53	3.68
εx [nm-rad]	15.6	139.2	176.8
ηx [m] (at interaction)	0.800	-1.038	-1.671
ηx [m] (at detector)	0.248	0.430	0.560

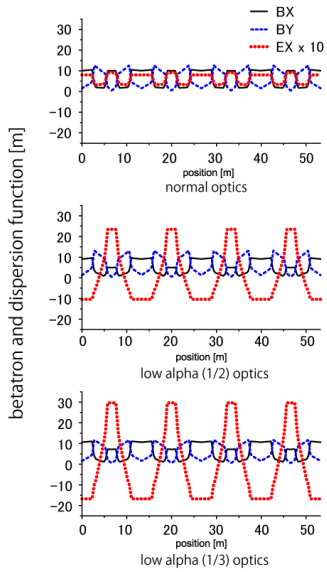

Figure 2: Horizontal and vertical betatron functions and dispersion function of (top) normal optics, (middle) low alpha(1/2) optics and (bottom) low alpha (1/3) optics .

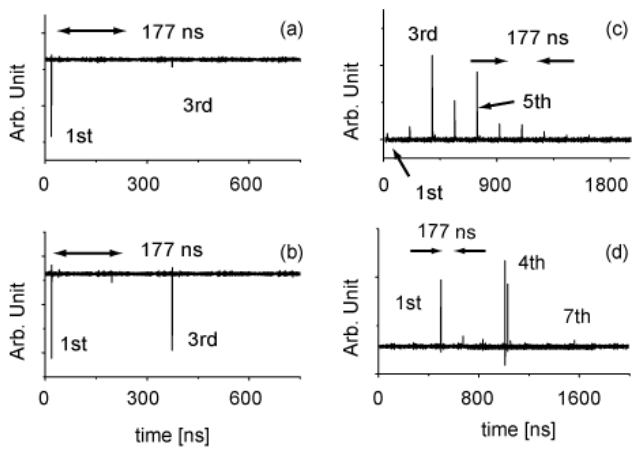

Figure 3: CSR signals of three diode detectors at the low-alpha optics. Revolution time of the ring is 177 ns. (a), (b), and (c) are with the low-alpha (1/2) optics and a laser pulse FWHM of 460 fs. Sensitivity ranges are (a) 11.0 - 16.6 cm^{-1}, (b) 7.3 - 11.0 cm^{-1}, and (c) 3.7 - 5.7 cm^{-1}. (d) is with low-alpha (1/3) optics and a laser pulse FWHM of 1 ps. Sensitivity range is 7.3 - 11.0 cm^{-1}.

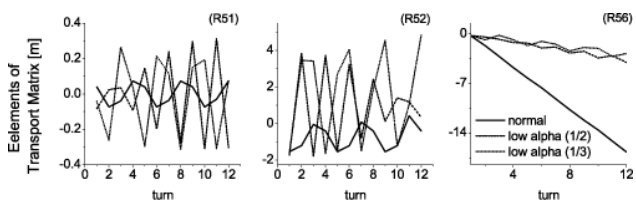

Figure 4: Development of R_{51}, R_{52} and R_{56} elements of transport matrices at each turn at normal and two low-alpha optics.

In the low-alpha (1/2) optics, the betatron tune is close to a half integer. Thus, the intermittent CSR emission was expected to be related to the betatron motion. To confirm this, we tried the same experiment with the low-alpha (1/3) optics. Because of the limited beam time, CSR was observed only at the middle frequency range. The result is shown in Fig. 3 (d). The CSR is intense at every third arrival, the first and fourth. Weak CSR is also observed at the seventh arrival, despite the absence of CSR at the fifth and sixth.

LINEAR BEAM DYNAMICS

The evolution of the dip structure is simulated based on linear beam dynamics theory. The transport matrix for the *n*th arrival at the source point can be written as

$$R^{(n)} = R_1 R_C^{(n-1)} \quad (2)$$

where $\boldsymbol{R}_1$ and $\boldsymbol{R}_C^{(n-1)}$ are the matrices from the interaction point to the source point, and n-1 full revolutions from the interaction point, respectively. It can be shown that the elements of $\boldsymbol{R}_C^{(n)}$ are related to the momentum compaction factor α_C as follows,

$$R_{C56}^{(n)} = n\alpha_C L - [\eta_x^* R_{C51}^{(n)} + \eta_{x'}^* R_{C52}^{(n)}] \quad (3)$$

where L, η_x^*, and $\eta_{x'}^*$, are the circumference of the storage ring, the momentum dispersion function, and its derivation at the start point of the transport matrix, respectively. Figure 4 shows the turn-by-turn developments of R_{51}, R_{52}, and R_{56} of the three beam optics, which start from the interaction point. We can see R_{51} and R_{52} oscillate at the betatron tune ν. Oscillation amplitudes are larger at the two low-alpha optics than at the normal optics. The absolute value of R_{56} also oscillates at the betatron tune with increasing turn-by-turn. In the case of low-alpha optics, the increase of the absolute value is suppressed, and the amplitude of the oscillation increases with increasing η_x^* and $\eta_{x'}^*$.

The change in the longitudinal position of an electron at the source point, Δz, was expressed by a linear equation,

$$\Delta z = R_{51} x_0 + R_{52} x_0' + R_{56}[\delta_0 + \Delta\delta(z)] \quad (4)$$

where x_0, x'_0, and δ_0 are the displacement and the derivation from the reference orbit in the horizontal plane, and the energy deviation before the interaction, which are Gaussian distributed with root mean square values of the beam size, the angular divergence at the interaction point and the energy spread. $\Delta\delta(z)$ is the energy change produced by the laser interaction, whose absolute value is much larger than δ_0.

The technique 'laser bunch slicing' makes two regions on the electron bunch; fragments and a low density region as shown in Fig. 5. The fragments of the modulated electron incline gradually according to α_C. When the momentum dispersion function at the interaction point is not zero, the fragments oscillate at betatron tune via longitudinal slippage due to R_{51} and R_{52}. It means the incline of the fragment on the longitudinal phase space oscillates according to R_{56} in eq. (3). On the other hand, the incline of low density region is proportional to α_C, which is independent to betatron tune. However, the unmodulated electrons nearby the low density region oscillate at betatron tune due to R_{51} and R_{52}. It results in the oscillation of electron density of the low density region. Both the oscillations of fragments and electron density at a low density region can induce the transverse-longitudinal effect. According the numerical simulation (results is not shown here), the latter effect is significant in this experiment.

The transverse-longitudinal coupling effect will be of great importance in advanced accelerators for short electron bunch such as storage ring with low-alpha or isochronous optics or energy recovery linacs [4]. In such accelerators, the bunch shape depends not only on the longitudinal dynamics but also on the transverse dynamics. This experiment also demonstrated that THz CSR measurement using several diode detectors sensitive to different frequency ranges is a powerful tool for observing evolution of longitudinal micro-structures.

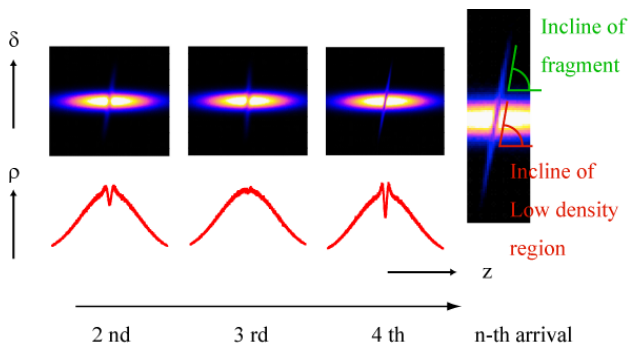

Figure 5: An example of evolution of fragments and a low density region in longitudinal phase space (upper) and its corresponding longitudinal dip formation (lower). The horizontal axis is an arrival order after the revolutions

REFERENCES

[1] e.g. Y. Shoji, Phys. Rev. ST Accel. Beams 7 (2004) 090703.
[2] M. Shimada et al., Phys. Rev. Lett. 103 (2009) 144802.
[3] M. Shimada et al., Jpn. J. Appl. Phys. 46 (2007) 7939.
[4] S. Sakanaka et al., in these proceedings, TUPE091.